Assessment of the corrected CMOD6 GMF using scatterometer data

Anis Elyouncha[1], Xavier Neyt[1], Ad Stoffelen[2] and Jeroen Verspeek[2]

[1]Royal Military Academy, 30 Av de la Renaissance, Brussels, Belgium

[2]Royal Netherlands Meteorological Institute, Utrechtseweg 297, De Bilt, Netherlands

ABSTRACT

An assessment of the agreement between the ERS scatterometers (ERS-1 and ERS-2) and the Metop scatterometers (ASCAT-A and ASCAT-B) is essential for the consistency of the C-band scatterometry dataset. ERS-1, ERS-2, ASCAT-A and ASCAT-B are C-band fan-beam radar scatterometers covering a range of common incidence angles. During these C-band scatterometry missions, different calibration campaigns have been carried out mainly relying on active ground transponders and natural distributed targets such as the rainforest. Additionally, these missions differ in time with some overlapping periods. Therefore, an assessment of the agreement between ERS and ASCAT measurements is an important and challenging task. This assessment is usually performed over the rainforest but only considering the common incidence angles. In order to perform the comparison over the whole incidence angle range of both radars, a Geophysical Model Function (GMF) is needed. An empirical correction of the CMOD5.n GMF has been suggested recently by KNMI resulting in a new GMF called CMOD6. This correction was derived from the comparison of the ASCAT backscatter measurements and the CMOD5.n model. Taking ASCAT's measurements as reference, the differences between the CMOD5.n and ASCAT measurements were attributed to GMF errors. Additionally, an overview of the existing C-band models is given. The comparison of these models shows relatively large differences. The aim of this paper is the assessment of the CMOD6 GMF using ERS-1 and ERS-2 ocean backscatter measurements and the validation of the applicability of the corrected GMF to the whole C-band scatterometry dataset. Finally, a method is suggested to calibrate the residual bias of all the C-band scatterometers w.r.t CMOD6. It is shown that after calibration a consistent scatterometer data model is obtained.

1. INTRODUCTION

The multiple C-band scatterometer missions have been providing a considerable amount of data spanning a long time period exceeding 25 years. These missions carried different instruments and used different calibration strategies. Therefore, consistent C-band scatterometer data is now an important concern and a great challenge. The wind retrieval from the backscatter measurements is performed using a Geophysical Model Function (GMF) which is an essential part of the scatterometry. The development and validation of the GMF has drawn the attention of many researchers in the field for the last three decades. These research efforts produced several empirical GMFs, based on the similar mathematical formulation, but differing in the empirical coefficients. However, a consistent data model requires a unified GMF for the C-band scatterometers series, applicable over full ERS/ASCAT incidence angle range [18^o-66^o].

The issue is that, since the GMFs are constructed empirically they are instrument/dataset dependent. For instance, the GMFs based on ERS data are not applicable to high incidence angles and GMFs based on only ASCAT data not to low incidence angles. The extrapolation of the GMFs at low and high incidence angles has shown large discrepancies with data. This does not provide good results, thus calibration coefficients are often applied to backscatter before wind retrieval. Therefore, a new GMF has been proposed, based on a correction of the CMOD5n model. The strategy adopted is an incidence-angle correction of the CMOD5n (developed for ERS) using ASCAT data (well calibrated). The corrected model is called CMOD6.[1]

The objective here is, first, to compare the different existing C-band GMFs in order to find the C-band GMF that best fits the ERS and ASCAT data and that is valid over the whole incidence angle range of ERS and Metop scatterometers i.e., from 18 to 66 degrees. The C-band GMF need also to be valid for the whole wind speed range measured by the two radars.

Further author information: (Send correspondence to Anis Elyouncha) E-mail: anis.elyouncha@elec.rma.ac.be, Telephone: +32 2 742 6665

First, the C-band scatterometers are briefly described and their differences are highlighted. Second, an overview of the existing C-band GMFs is given, also highlighting their discrepancies. Third, a comparison of the scatterometer data to the CMOD5n, CMOD5na and CMOD6 is performed using the NOC method (see section 6.1). Finally, the residual biases in the backscatter data are corrected to fit the CMOD6 model which yields a consistent dataset.

2. C-BAND SCATTEROMETERS AND THEIR DIFFERENCES

A scatterometer is a real aperture radar that is designed to measure the backscattered power of distributed targets from different azimuth angles. C-band scatterometers such as ERS and Metop radars operate at carrier frequency 5.3 GHz and 5.255 GHz respectively. ERS and Metop radars both use three fan-beam antennae (called fore, mid and aft) looking in three different azimuth angles (45, 90 and 135). ERS-1 and ERS-2 scatterometers are identical in design just as Metop-A and Metop-B scatterometers are. However, the two series of scatterometers (ERS and Metop) differ in some aspects as it is described below.

As mentioned above, The GMF development is based on scatterometer data. Thus, though ERS/AMI and Metop/ASCAT scatterometers are very similar radars (both real aperture, fan beam radars operating at the same frequency and polarization (VV)), they have some differences which may have an impact on the GMF development based on their data. The difference in the carrier frequency is very small (45 MHz) so is not considered. For instance ERS and ASCAT differ in the spatial resolution (due mainly to the difference in the bandwidth).[2] They also differ in the radiometric resolution, it has been shown[3] that ASCAT scatterometers have lower Noise Equivalent Sigma Zero (NESZ) and lower Kp than ERS-2 scatterometer. Finally, the difference in the illuminated incidence angle range hinders the inter-calibration and the development of a unified GMF. ERS swath extends from 18 to 57 deg while ASCAT swath extends from 25 deg to 65 deg. That is the two swaths are shifted by approximately 7 degrees.

Scatterometers differ also in the measurement space as explained hereafter. The three-dimensional visualization of the C-band GMF and the backscatter triplets, where the x, y and z axis represent fore, aft and mid beam backscatter, forms a cone surface.[4] Analysis of this cone surface is very useful and often used to assess and detect anomalies in backscatter measurements. Figure 1 shows a projection of the cone surface on the mid, fore=aft plane. It can be noticed from figure 1 that ERS-2 is characterized by a non-linearity (saturation) at low backscatter. This is a known ERS-2 anomaly,[5] although its origin is not yet totally understood. This anomaly is not present in the other scatterometer's measurements (ERS-1, ASCAT). This might have had an impact on the GMFs development based on ERS-2 data.

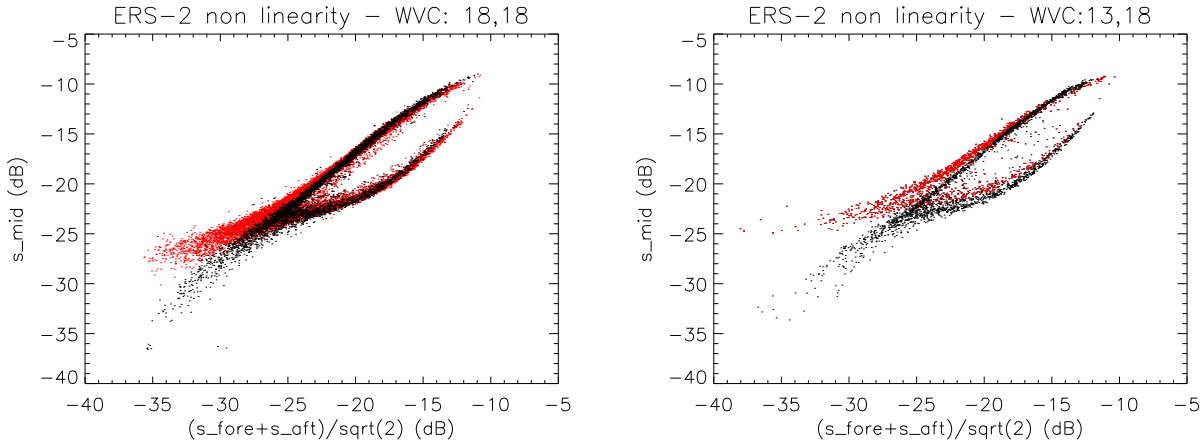

Figure 1. ERS-2 non linearity; Red: ERS-2; Black: ERS-1 (left), ASCAT (right)

3. THE C-BAND GMFS

3.1 Overview

A Geophysical Model Function (GMF) is an empirical relationship relating the backscatter to the wind vector given by:

$$\sigma 0 = f(v, \phi, \theta, pp, \lambda) \tag{1}$$

Where $\sigma 0$ is the Normalized Radar Cross-Section (NRCS) also called backscatter or backscattering coefficient, v is the wind speed at a reference altitude of 10 m, ϕ is the relative wind direction with respect to azimuth look angle i.e., $\phi = 0$ means up wind, θ is the radar incidence angle, pp is the polarization, and λ is the radar wavelength.

All the C-band GMFs have a similar mathematical formulation which is based on a harmonic decomposition of the backscatter signal as function of the relative wind direction (see figure 4).

$$\sigma 0(\theta, v, \phi) = B_0(\theta, v)[1 + \sum_{k=1}^{N} B_k(\theta, v) cos(k\phi))]^p. \tag{2}$$

The B_0 and B_k coefficients are determined empirically by matching the scatterometer measurements with reference winds. These reference winds can be measured by another source e.g., buoy, aircraft, etc. or provided by a Numerical Weather Prediction (NWP) model. Thus, since B_0 and B_k coefficients are dependent on the backscatter and the wind dataset used, different GMFs are derived.

All the following existing C-band GMFs (CMOD4, CMOD-IFR2, CMOD5, CMO5n, CMOD5na, CMOD6, CMOD5.H, CMOD-RSS) are discussed and compared in this paper. The models previous to CMOD4 are not treated here. CMOD4 was derived by fitting ERS-1/AMI backscatter measurements to ECMWF analysis winds.[6] CMOD-IFR2 was derived by fitting ERS-1/AMI backscatter to collocated National Data Buoy Center (NDBC) buoy winds and ECMWF analysis winds.[7,8] CMOD4 and CMOD-IFR2 have been, for a long time, the basis for operational wind products provided by ESA and IFREMER respectively. CMOD5 was derived using ERS-2/AMI backscatter data and ECMWF analysis winds.[5] The CMOD5 was developed to correct for some deficiencies of the CMOD4 mainly at low and high wind speeds. CMOD5n was developed to take into account the difference between real winds (atmospheric stability dependent) and neutral winds.[9] Another C-band model, based on ASCAT data, was developed in 2013 by the Remote Sensing Systems (http://www.remss.com/missions/ascat), this model is called here CMOD-RSS. For the construction of CMOD-RSS, the wind speeds were provided by SSMI and windsat radiometers while the wind directions were obtained from CCMP. The CMOD5.H[10] is a refinement of the CMOD5n to correct the bias at extreme wind speeds. The development of the CMOD5.H is based on the IWRAP airborne scatterometer / Doppler radar.

CMOD5na[11] is obtained by applying an incidence-angle correction to the B_0 coefficient of CMOD5n (developed for ERS) using the well calibrated ASCAT data as a reference. The underlying assumption is that the bias between ASCAT and CMOD5n are attributed to the GMF which has not been validated at the high ASCAT incidence angles ($56 - 66$ degree). However, the comparison of CMOD5na and ERS data has shown a large bias at low incidence angles. This finally has motivated the development of CMOD6 to take into account the whole incidence angle range of the C-band scatterometers (ERS and ASCAT). This is also a correction of the B_0 coefficient of CMOD5n, the other coefficients (B_1 and B_2) are kept the same (see section 6).

3.2 GMF comparison

Since the C-band GMF's are developed using different datasets. Either reference winds and backscatter data are different or using the same reference winds with different backscatter measurements (scatterometer). Additionally, the C-band scatterometers have different characteristics in terms of resolution, noise, etc. Therefore, it is expected (but not desired) that these GMFs show different behaviours of the backscatter as function of wind speed, wind direction and incidence angle.

3.2.1 Backscatter as a function of incidence angle

Figures 2 shows the NRCS as a function of incidence angle for a given wind speed (7.5 m/s) and relative direction (up wind) for all the CMOD GMFs discussed above. First, it is noticeable the departure of the CMOD4 and CMOD5 from the group of GMFs. This departure increases with incidence angle. These two models are known to be biased.[5,12] Note, that, all the GMFs are extrapolated over the whole incidence angle range of ERS and ASCAT i.e., from 18 to 66. For instance, CMOD-RSS was built for ASCAT so is not meant to be used at incidence angles lower than 25, but it is extrapolated here for comparison. This explains the large discrepancy of the latter from the other GMFs at incidence angles lower than 30 deg.

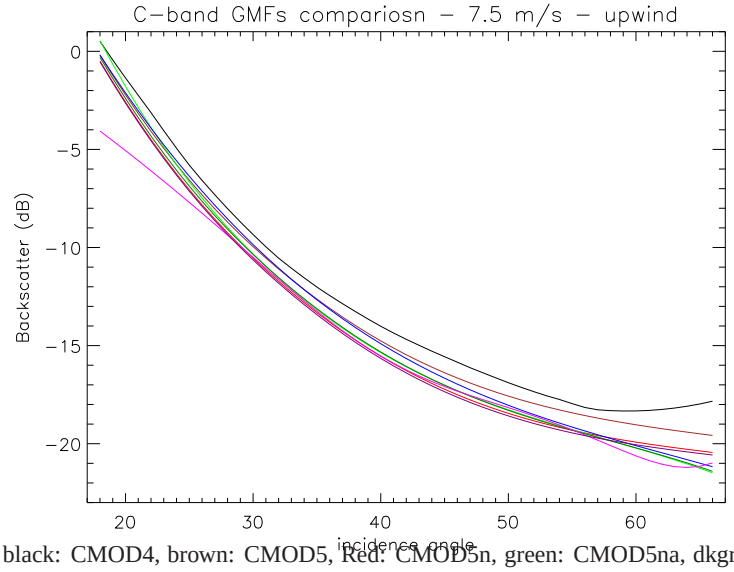

Figure 2. GMF comparison; black: CMOD4, brown: CMOD5, Red: CMOD5n, green: CMOD5na, dkgreen: CMOD6, blue: CMOD-IFR2, magenta: CMOD-RSS, purple: CMOD5H

3.2.2 Backscatter as a function of wind speed

Figure 3 depicts the NRCS as a function of wind speed for a given incidence angle (40 deg) and relative wind direction (up wind). First, there is a clear departure of CMOD4 and CMOD-IFR2 from the the rest of the group of GMFs at wind speeds above 18 m/s. This is due to the change in the power law relating the B_0 coefficient and the wind speed since CMOD5 at high wind speed regime.[5] It is also interesting to notice that CMOD4 has no response below a cut-off wind speed of approximately 1 m/s. Generally, the models agree quite well in the 3-15 m/s wind speed regime and disagree out of his regime.

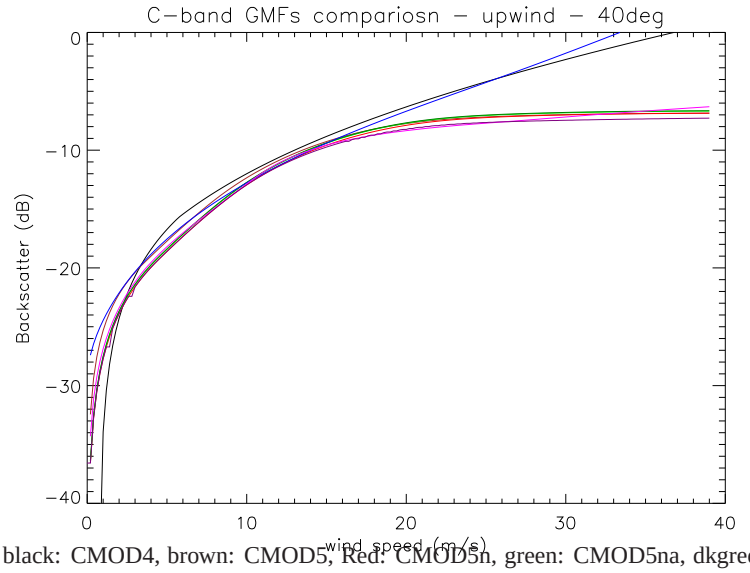

Figure 3. GMF comparison; black: CMOD4, brown: CMOD5, Red: CMOD5n, green: CMOD5na, dkgreen: CMOD6, blue: CMOD-IFR2, magenta: CMOD-RSS, purple: CMOD5.H

3.2.3 Backscatter as a function of wind direction

Figure 4 depicts the NRCS as a function of the wind direction relative to the beam for a given incidence angle (40 deg) and wind speed (7.5 m/s). The figure confirms the departure of the CMOD4, CMOD-IFR2 and the CMOD5 from the rest of the group at all wind directions. The other GMFs (CMOD5n, CMOD5na, CMOD6 and CMOD-RSS) are relatively close. It can be also noticed that the difference between some GMFs is wind direction dependent indicating a difference in their B_1 and B_2 coefficients.

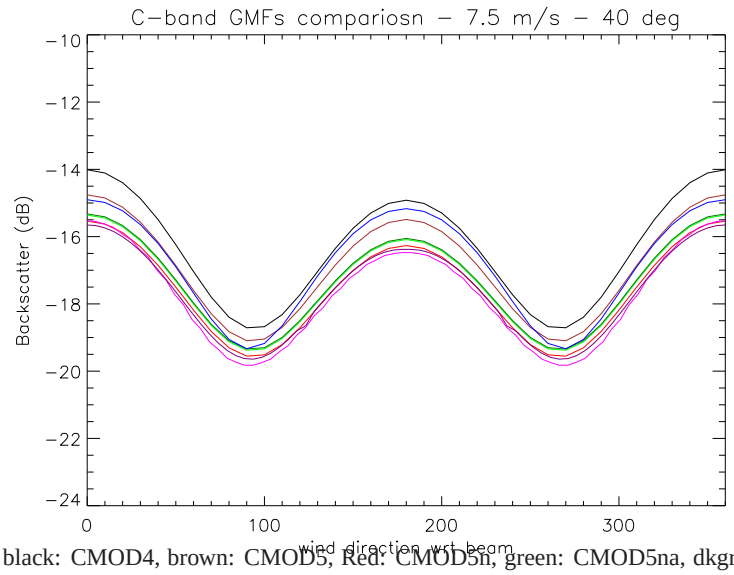

Figure 4. GMF comparison; black: CMOD4, brown: CMOD5, Red: CMOD5n, green: CMOD5na, dkgreen: CMOD6, blue: CMOD-IFR2, magenta: CMOD-RSS, purple: CMOD5.H

To conclude, there are relatively large differences between the models. These differences are largest at extreme incidence angles and wind speeds and may reach 0.6 dB. This is a relatively large difference compared to the scatterometer accuracy requirement i.e., 0.2 dB. For the ERS and ASCAT calibration (see section 6) only CMOD5n, CMOD5na and CMOD6 are considered.

4. IMPACT OF THE INSTRUMENT ANOMALIES ON THE GMF

The effect of the difference between the scatterometers characteristics or more specifically the ERS-2 non-linearity, on the GMF is illustrated in figures 5 and 6. The models are simulated at the farthest Wind Vector Cell (WVC) from nadir or the largest incidence angle (55^o) where the backscatter is the lowest and the effect is most pronounced. The wind speed extends from 0 to 30 m/s.

In the measurement space, this is illustrated by the projection of the cone on the mid-fore plane (figure 5). Note that, for clarity, only the upper layer of the cone, which corresponds to the upwind direction, is depicted. It can be, clearly, noticed from the figure that the models that are based on ERS-2 data i.e., CMOD5, CMOD5n and CMOD6, show a non linear behaviour at low backscatter values and saturate at approximately -32 dB. Note also a slight improvement of CMOD5n and CMOD6 with respect to CMOD5. On the other hand, the models that are based on ERS-1 and ASCAT i.e., CMOD4, CMOD-IFR2 and CMOD-RSS respectively, show a linear behaviour over a larger backscatter range and extend toward much lower backscatter values.

Similar conclusion is driven from figure 6 which depicts the backscatter as a function of wind speed. It can be noticed from the figure that the models that are based on ERS-2 data i.e., CMOD5 and CMOD5n, thought there is a slight improvement with CMOD5n, are truncated at certain lower backscatter threshold of approximately -32 dB. On the other hand, the models that are based on ERS-1 and ASCAT extend toward lower backscatter values for a given wind speed. This is in line with the figure 1 illustrating the same effect with the measured data. This is also in agreement with the fact that

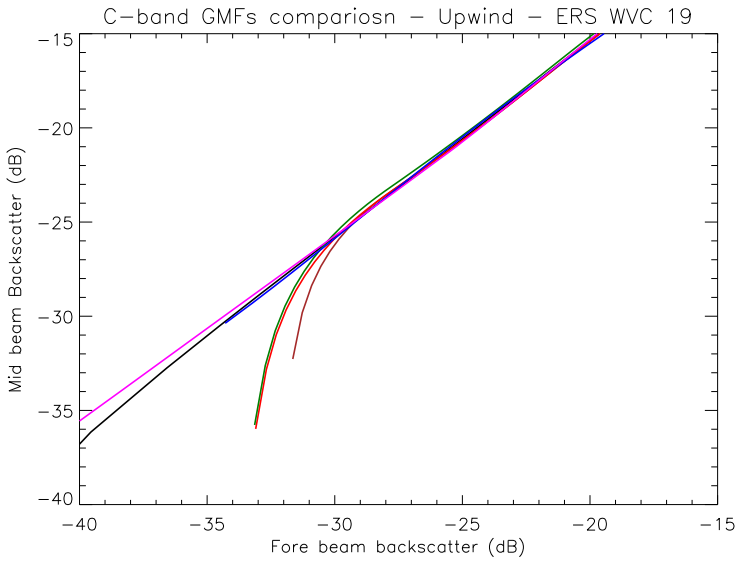

Figure 5. ERS-2 non linearity impact on the GMF; WVC 19 [$\theta^f = 55, \theta^m = 45$]; CMOD cone projection; black: CMOD4, brown: CMOD5, blue: CMOD-IFR2, green: CMOD5, red: CMOD5n, magenta: CMOD-RSS

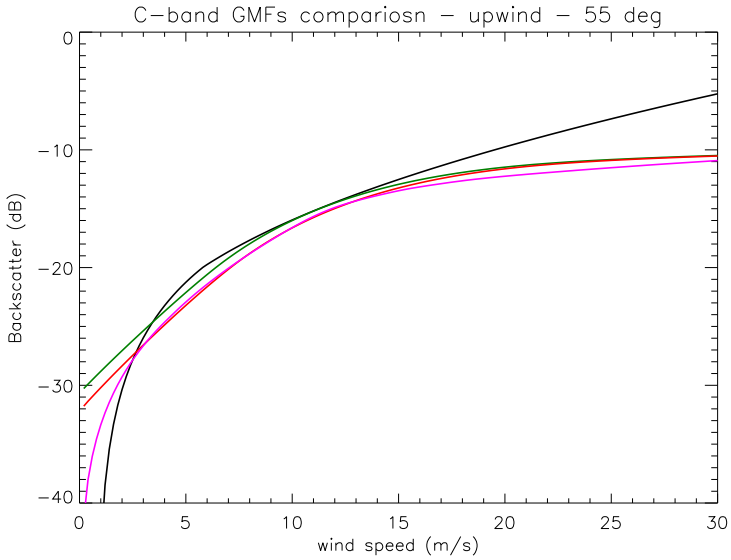

Figure 6. ERS-2 non linearity impact on the GMF; NRCS as a function of wind speed; black: CMOD4, green: CMOD5, red: CMOD5n, magenta: CMOD-RSS

ASCAT has a lower Noise Equivalent Sigma Zero (NESZ) than ERS-2. This indicates that the instrument/data anomalies are transferred to the GMF derived from these data.

5. CMOD6 DEVELOPMENT

The underlying assumption for the development of CMOD6 is that ASCAT is absolutely (using ground transponders) well calibrated, thus taken as a reference. The assumption is based on the fact that ASCAT benefits from regular absolute calibration campaigns using active transponders.[13] Moreover, validation studies have demonstrated the accuracy of ASCAT data e.g.,.[13,14] However, a comparison of the ASCAT backscatter and the CMOD5n yields large differences at

high incidence angles. CMOD5n was developed for ERS, thus is not validated at high incidence angles. Therefore, the incidence-angle dependent bias between ASCAT backscatter and the CMOD5n GMF are attributed to the GMF errors. The residual beam-dependent biases are attributed to instrument calibration, this bias correction is applied to the backscatter.

Initially, the NOC bias of ASCAT w.r.t CMOD5n were fitted with a 3^{rd} order polynomial (equation 4) yielding CMOD5na.[15] The CMOD5na is derived from CMOD5n as follows[15]

$$\sigma 0^{CMOD5na}(\theta) = \sigma 0^{CMOD5n}(\theta) B_0^{corr5}(\theta) \tag{3}$$

Where

$$B_0^{corr5}(\theta) = a_0 + a_1\theta + a_2\theta^2 + a_3\theta^3 \tag{4}$$

and $a_0 = 5.7236425879$, $a_1 = -0.4226930560$, $a_2 = 0.0105605079$, $a_3 = -0.0000864832$.

This fits well the ASCAT NOC bias for the ASCAT incidence angle range (see figure 7). However, the fit at the lower ERS incidence angles is not valid (see figure 8). Therefore, a new fit on the same ASCAT data was performed, but with a 5^{th} order polynomial (equation 6) with boundary condition ($dB0/d\theta = 0$) at $\theta = 20^o$ yielding CMOD6. The extra boundary condition forces a flat correction at the lower incidence angles which allows the model to be also valid for ERS.

Thus, to account for ERS low incidence angles, CMOD5n is corrected to become CMOD6. The CMOD6 is derived from CMOD5n as follows

$$\sigma 0^{CMOD6}(\theta) = \sigma 0^{CMOD5n}(\theta) B_0^{corr6}(\theta) \tag{5}$$

Where the B_0^{corr6} for CMOD6 is

$$B_0^{corr6}(\theta) = a_0 + a_1\theta + a_2\theta^2 + a_3\theta^3 + a_4\theta^4 + a_5\theta^5 \tag{6}$$

and $a_0 = 1.00557711e-02$, $a_1 = 2.63968952e-02$, $a_2 = -1.36487705e-03$, $a_3 = 2.33507248e-05$, $a_4 = 1.20736387e-07$, $a_5 = -4.60930473e-09$.

6. SCATTEROMETER CALIBRATION

6.1 NOC method

The NWP Ocean Calibration (NOC)[16,17] consists in computing the difference between the measured and the simulated backscatter, averaged over wind direction and speed. This is a well established method usually used to compute the bias between scatterometer data and a reference GMF (fed by reference background winds). Here the reference GMF is CMOD5n and the reference background winds are the ECMWF analysis winds. The method is used here, first, to compare the scatterometer data to CMOD5n, CMOD5na and CMOD6 GMFs in order to determine which fits the best the data. The results of the NOC are illustrated by showing the NOC bias ($B_0^{meas} - B_0^{sim}$) w.r.t CMOD5n for ERS-1 and ERS-2. CMOD5na and CMOD6 bias i.e. $B_0^{CMOD5na} - B_0^{CMOD5n}$ and $B_0^{CMOD6} - B_0^{CMOD5n}$ respectively, are also shown for comparison. Second, an incidence-angle-dependent bias w.r.t the "best" GMF is computed for each beam. Finally, this bias is applied to the measured backscatter.

Figure 7 depicts the bias between ASCAT data and the CMOD5n GMF obtained using the NOC method. One can notice a large bias up to 0.7 dB at high incidence angles.This is more likely due to inaccuracies in the GMF rather than to ASCAT instrument calibration issues.[13,14] The CMOD5na and CMOD6 are also over-plotted. Obviously, CMOD5na and CMOD6 fits much better ASCAT, which was expected since this was the purpose of deriving CMOD5na and CMOD6.

Similarly, NOC is applied to ERS-1 and ERS-2 data, this yields the result (NOC bias w.r.t CMOD5n) depicted in figure 8. The figure shows that CMOD6 is, on average, the closest GMF to ERS data. The remaining residual (generally small) biases w.r.t CMOD6 (reference GMF) are corrected at each WVC (calibration). The correction of the beam- and WVC-dependent biases, should yield a good agreement between ERS data and ASCAT data (CMOD6).

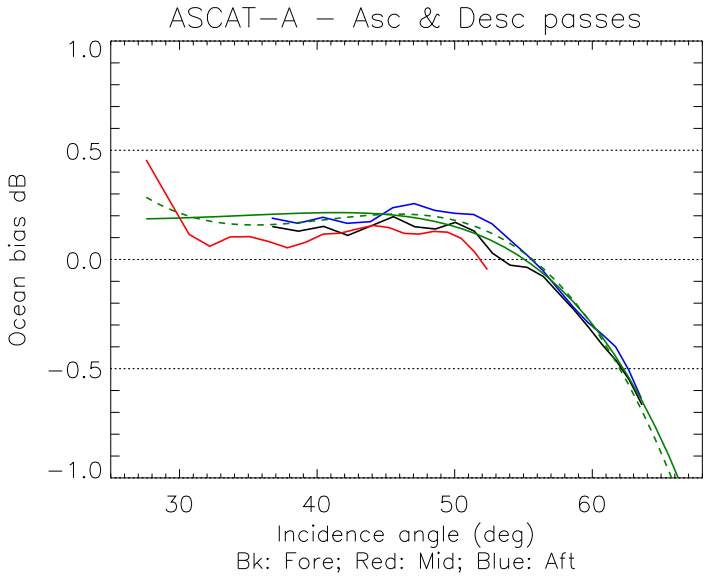

Figure 7. NOC bias w.r.t CMOD5n (before calibration); January 2009; dashed green: CMOD5na-CMOD5n, solid Green: CMOD6-CMOD5n

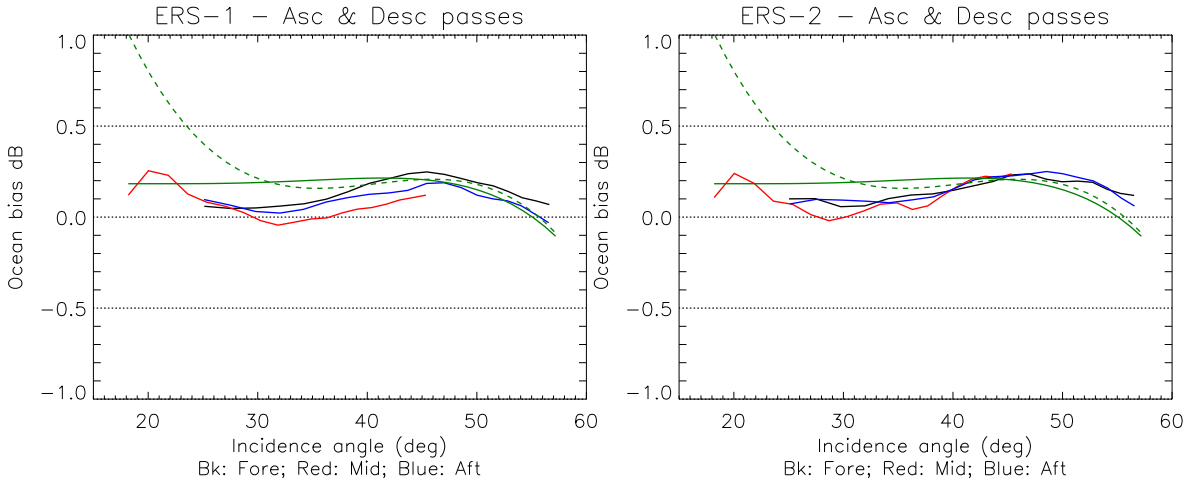

Figure 8. NOC bias w.r.t CMOD5n (before calibration); left: ERS-1 from 20-Mar to 03-Jun 1996; Right: ERS-2 from 20-Mar to 03-Jun 1996; solid green: $B0^{CMOD6} - B0^{CMOD5n}$, dashed green: $B0^{CMOD5na} - B0^{CMOD5n}$

6.2 Inter-calibration methodology

The inter-calibration consists, first, in a comparison of the backscatter measured by each scatterometer's antenna as a function of incidence angle. From this comparison a beam and incidence-angle-dependent bias is determined. The difference in backscatter is attributed to a difference in the antenna gain pattern. One of the two scatterometers is considered as a reference and the other is corrected to fit the reference.

For the inter-calibration of ERS-1 and ERS-2[18] and Metop-A and Metop-B,[19] either the rainforest or the ocean model are used successfully, i.e., both yield a similar results. However, For inter-calibrating Metop and ERS scatterometers, as the range of incidence angles spanned by each radar is different, the rainforest is not applicable over the whole incidence angle range and the ocean model is not accurate when is extrapolated in incidence angle as discussed above.

Therefore, in the case of ERS/ASCAT inter-calibration a C-band GMF that is valid over the whole incidence range is preferred. Here, the CMOD6 GMF is used as reference for inter-calibration. Note, that this is equivalent to considering

ASCAT as a reference.

6.3 Inter-calibration results

Same correction method (NOC) is applied to ERS-1, ERS-2, ASCAT-A and ASCAT-B. Figures 9 shows the NOC bias of ERS-1 and ASCAT-A w.r.t CMOD5n. The results for ERS-2 and ASCAT-B are very similar, thus they are not shown. As expected, after calibration, the NOC bias follows closely the NOC bias of CMOD6 (solid green curve). That is to say, CMOD6 fits very well the calibrated ERS and ASCAT data.

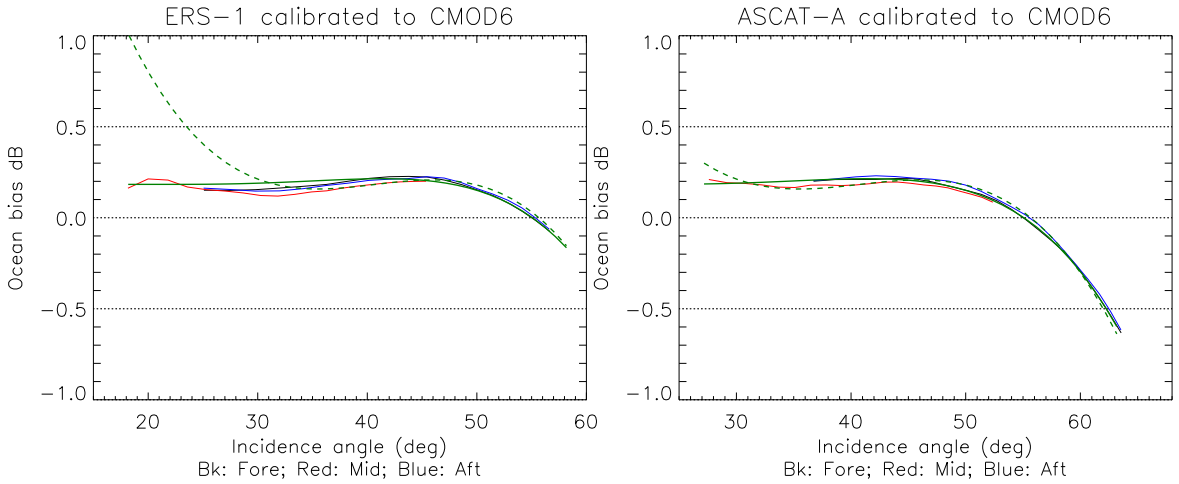

Figure 9. NOC bias w.r.t CMOD5n (after calibration); left: ERS-1 from 20-Mar to 03-Jun 1996; Right: ERS-2 from 20-Mar to 03-Jun 1996; Black: Fore; Red: Mid; Blue: Aft; solid green: $B0^{CMOD6} - B0^{CMOD5n}$, dashed green: $B0^{CMOD5na} - B0^{CMOD5n}$

Finally, the residual NOC bias of the four scatterometers together w.r.t to CMOD6 are shown in figure 10. As can be noticed, after calibration of each scatterometer data to CMOD6, the residuals are very small over all incidence angles which yields a consistent C-band backscatter down to 0.1 dB.

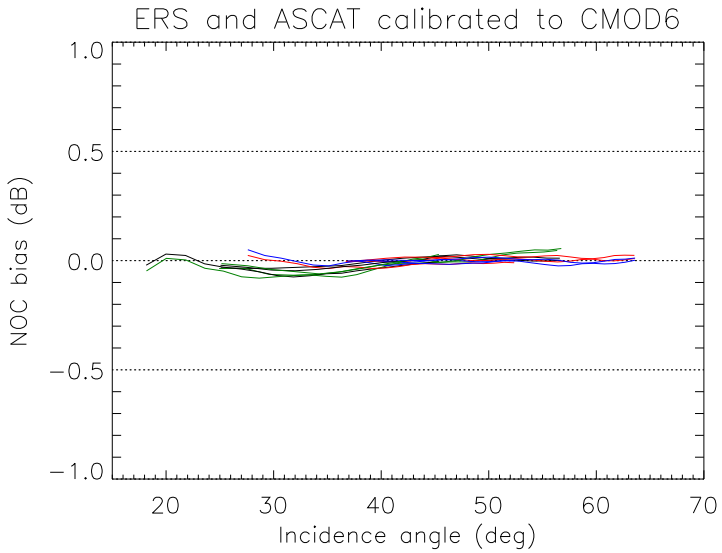

Figure 10. NOC bias w.r.t CMOD6 (after calibration); Black: ERS-1; Green: ERS-2; Red: ASCAT-A, Blue: ASCAT-B

7. CONCLUSION

The comparison of the existing C-band GMFs revealed large differences particularly at low/high incidence angles and wind speeds. This comparison has also shown that CMOD6 is the best candidate for C-band data given the current calibration. CMOD6 fits well ERS and ASCAT over all incidence angles, winds and directions with the lowest bias. Finally, note that the development of CMOD6 assumes that ASCAT is well calibrated. Thus, calibrating ERS data w.r.t CMOD6 is equivalent to calibrating ERS to ASCAT data. It is shown (see figure 10) that after correcting the residual biases of the four scatterometers w.r.t CMOD6, a consistent (within 0.1 dB) C-band scatterometer data is obtained. Finally, Note that CMOD6 has inherited from CMOD5n the impact of the ERS-2 non-linearity as discussed in section 2. Thus, an additional correction is needed to take into account this effect. This is possible by using CMOD-RSS, which is based on ASCAT data, in the low backscatter range.

8. ACKNOWLEDGEMENT

Data was provided by ESA, Eumetsat and we would like to thank these institutes.

REFERENCES

[1] A. Elyouncha and X. Neyt. Assessment of the corrected cmod5.n ocean backscatter model using ers scatterometer data. https://coaps.fsu.edu/scatterometry/meeting/past.php, 2015.

[2] A. Elyouncha and X. Neyt. Comparison of the spatial and radiometric resolution of ERS and Metop C-band radars. In *Proceedings of SPIE Remote sensing, Amsterdam, 2014*, September 2014.

[3] A. Elyouncha and X. Neyt. Analysis of C-band spaceborne scatterometer thermal noise. In *Proceedings of SPIE Remote sensing, Amsterdam*, September 2014.

[4] A. Stoffelen and D. Anderson. Scatterometer data interpretation: Measurement space and inversion. *Journal of atmospheric and oceanic technology*, 14(6):1298–1313, February 1997.

[5] H. Hersbach, A. Stoffelen, and S. de Haan. An improved C-band scatterometer ocean geophysical model function: CMOD5. *Journal of Geophysical Research: Oceans*, 112(3):1978–2012, March 2007.

[6] A. Stoffelen and D. Anderson. Scatterometer data interpretation: Estimation and validation of the transfer function CMOD4. *Journal of atmospheric and oceanic technology*, 14(6):1298–1313, February 1997.

[7] Y. Quilfen, B. Chapron, T. Elfouhaily, K. Katsaros, and J. Tournadre. Observation of tropical cyclones by high-resolution scatterometry. *Journal of geophysical research*, 103(4):7767–7786, April 1998.

[8] A. Bentamy, P. Queffeulou, Y. Quilfen, and K. Katsaros. ocean surface wind fields estimated from satellite active and passive microwave instruments. *IEEE Transactions on Geoscience and Remote Sensing*, pages 2469–2486, 1999.

[9] H. Hersbach. CMOD5.N a C-band geophysical model function for equivalent neutral wind. Technical report, ECMWF, April 2008. ECMWF technical Memorandum 554.

[10] Seubson Soisuvarn, Zorana Jelenak, Paul S. Chang, Suleiman O. Alsweiss, and Qi Zhu. CMOD5.H a high wind geophysical model function for c-band vertically polarized satellite scatterometer measurements. *IEEE Transactions on Geoscience and Remote Sensing*, 51(6):3744–3760, June 2013.

[11] J Verspeek, A Stoffelen, A Verhoef, and M Portabella. Improved ascat wind retrieval using NWP ocean calibration. *IEEE Transactions on Geoscience and Remote Sensing*, 50(7):2488–2494, July 2012.

[12] H. Hersbach, A. Stoffelen, and S. de Haan. Comparison of C-Band scatterometer CMOD5.N equivalent neutral winds with ECMWF. *Journal of Atmospheric and Oceanic Technology*, 27:721–736, April 2010.

[13] C. Anderson, J. Figa, H. Bonekamp, J. Wilson, J. Verspeek, A. Stoffelen, and M. Portabella. Validation of backscatter measurements from the advanced scatterometer on Metop-A. *J. Atm. Oceanic Technol.*, 29:77–88, February 2012.

[14] J.A. Verspeek, A. Stoffelen, M. Portabella, H. Bonekamp, C. Anderson, and J. Figa. Validation and calibration of ASCAT using CMOD5.n. *IEEE Transactions on Geoscience and Remote Sensing*, 48(1):386–395, July 2010.

[15] J. Verspeek, A. Stoffelen, A. Verhoef, M. Portabella, and J. Vogelzang. ASCAT-B ocean calibration and wind product. In *2012 EUMETSAT Meteorological Satellite Conference (2012), Sopot, Poland*, September 2012.

[16] A. Stoffelen. A simple method for calibration of a scatterometer over the ocean. *Journal of atmospheric and oceanic technology*, 16(2):275–282, February 1999.

[17] J. Verspeek. Scatterometer calibration tool development. Technical Report SAF/OSI/CDOP/KNMI/TEC/TN/163, KNMI, March 2006.

[18] A. Elyouncha and X. Neyt. A method for cross-comparison of scatterometer data using natural distributed targets: application to ERS-1 and ERS-2 data during the tandem mission. In *Proc. SPIE 8532, Remote Sensing of the Ocean, Sea Ice, Coastal Waters, and Large Water Regions 2012*, October 2012.

[19] A. Elyouncha and X. Neyt. Inter-calibration of metop-a and metop-b scatterometers using ocean measurements. In *Proc. SPIE 8888, Remote Sensing of the Ocean, Sea Ice, Coastal Waters, and Large Water Regions 2013*, October 2013.